Antiviral activity of Molnupiravir precursor NHC against SARS-CoV-2 Variants of Concern (VOCs) and implications for the therapeutic window and resistance

Keywords: Molnupiravir, NHC, Anti-viral, ß-D-N4-hydroxicytidine, SARS-CoV-2, resistance

Running title: *In-vitro* activity of Molnupiravir against SARS-CoV-2 Variants of Concern

Tessa Prince[1,2], I'ah Donovan-Banfield[1,2], Hannah Goldswain[1], Rebekah Penrice-Randal[1], Catherine Hartley[1], Saye Khoo[2,3], Tom Fletcher[2,4], Julian A. Hiscox[1,2,5*]

[1]Institute of Infection, Veterinary and Ecological Sciences, University of Liverpool, UK.

[2]NIHR Health Protection Research Unit in Emerging and Zoonotic Infections, Liverpool, UK.

[3]Institute of systems, molecular and integrative biology, University of Liverpool, UK.

[4]Liverpool School of Tropical Medicine, Liverpool, UK.

[5]A*STAR Infectious Diseases Laboratories (A*STAR ID Labs), Agency for Science, Technology and Research (A*STAR), Singapore.

[*]Corresponding author: julian.hiscox@liverpool.ac.uk Tel: +44 (0)151 795 0222

Abstract

Several regulatory agencies have either licensed or given emergency use approval for treatment of patients at risk of developing severe COVID-19 with the anti-viral drug, Molnupiravir. Recent trials involving Molnupiravir suggested the drug was not as efficacious as earlier studies suggested. This study aimed to: (i) determine the effectiveness of the Molnupiravir active metabolite (NHC) against different SARS-CoV-2 Variants of Concern (VoCs), (ii) establish the therapeutic window of NHC in a human lung cell model, and (iii) and evaluate the genetic barrier to resistance. Dose response assays were performed in parallel to determine the IC50 (the concentration required to inhibit virus titre by 50%) of NHC against different variants. Human ACE-2 A549 cells were treated with NHC at different time points either before, during or after infection with SARS-CoV-2. Multiple passaging in the presence or absence of drug was used to evaluate whether resistance occurred. To obtain genomic information, virus was sequenced at regular intervals. After 20 passages in the presence of the drug, dose response assays and sequencing showed the virus did not appear to have developed resistance. The drug had equivalent activity against four VOCs ranging from 0.04 to 0.16µM IC50. The efficacy of the drug diminished when applied after 24 hours post-infection. Our results suggest that earlier administration in patients, perhaps pre- or post-exposure rather than symptom onset, would be a more effective treatment option.

47 **1.0 Introduction**

48 SARS-CoV-2 emerged in China in late 2019 and is the causative agent of the disease known
49 as COVID-19. While vaccination efforts have been largely successful in preventing severe
50 disease, many people worldwide remain unvaccinated. Additionally, important groups of
51 patients, such as those on immunosuppressive therapies, mount suboptimal responses to
52 vaccines (Kearns et al., 2021). For people in these categories, initially successful alternative
53 countermeasures such as monoclonal antibodies and protease inhibitors are declining in their
54 effectiveness as the virus evolves (Cox et al., 2022; Moghadasi et al., 2022). Therefore,
55 treatments that have longevity in the face of virus evolution are required.

56 Anti-virals can target either specific viral proteins or act non-specifically across the viral
57 genome. Three anti-virals for SARS-CoV-2 have been licensed in the UK:
58 Nirmatrelvir/Ritonavir (Paxlovid), Remdesivir and Molnupiravir (Haddad et al., 2022), each
59 with their own advantages and disadvantages.

60 Paxlovid is an oral combination therapy of protease inhibitors targeting the SARS-CoV-2
61 main protease (M^{pro}). It has been successfully used clinically, though must be used with care
62 due to its drug-drug interactions. However, there are some *in-vitro* indications that resistance
63 can develop to Nirmatrelvir (Jochmans et al., 2023; Zhou et al., 2022). The nucleoside
64 analogue Remdesivir incorporates into the viral RNA strand, and causes chain termination,
65 directly inhibiting the proteins involved in RNA synthesis (Kokic et al., 2021). However, the
66 drug must be given intra-venously, requiring a visit to hospital. Additionally, resistance to the
67 drug has also been shown to develop *in vitro* (Szemiel et al., 2021). Finally, another nucleoside
68 analogue, which acts to indirectly inhibit SARS-CoV-2 replication through the induction of
69 transition mutations (e.g. C -> U or G -> A changes) is Molnupiravir (Kabinger et al., 2021). This
70 results in error catastrophe during viral replication.

71 Molnupiravir is an orally bioavailable pro-drug that is converted enzymatically *in-vivo*
72 to its active form ß-D-N4-hydroxycytidine (NHC). Molnupiravir treatment reduces viral load
73 and block transmission in several animal models (Abdelnabi et al., 2021; Cox et al., 2021; Wahl
74 et al., 2021).

75 Molnupiravir has been evaluated in several large clinical trials for the treatment of
76 COVID-19. The MOVe-OUT trial held in the USA suggested a subtle effect of the drug with an
77 estimate of reduction in risk of hospitalisation or death from 9.7% to 6.8% in unvaccinated
78 individuals (about 30% reduction). In this trial 47.7% received the drug within 3 days or less
79 from symptom onset, the rest within 5 days. Molnupiravir administration resulted in faster
80 normalisation of clinical indicators compared to placebo, and those who received the drug
81 earlier had larger reductions in viral load compared to baseline (Jayk Bernal et al., 2022). A
82 post-hoc analysis of immunocompromised patients in the MOVe-OUT trial further found
83 Molnupiravir reduced incidence of hospitalisation or death (Johnson et al., 2023). The open-
84 label PANORAMIC trial from the UK has recently suggested that Molnupiravir, when given to
85 vaccinated individuals at a median of three days from symptom onset, did not significantly
86 reduce risk or hospitalisation/death, but did result in a faster self-reported time to recovery
87 and reduced viral load (Butler et al., 2022). The AGILE trial in the UK supported this result
88 suggesting a shorter time to PCR negativity and some moderate anti-viral activity in both
89 vaccinated and unvaccinated individuals compared to placebo, though the evidence was not
90 conclusive (Khoo et al., 2022). Finally, another Phase 2a double-blind, placebo controlled,
91 multicentre trial evaluated the safety and tolerability of the drug and found that 92.5% of
92 Molnupiravir treated patients achieved viral RNA clearance (measured by PCR) compared to
93 80.3% who received placebo. Likewise, isolation of live virus decreased after administration
94 of the drug (Fischer et al., 2021).

The development and assessment of anti-viral drugs is a notoriously long process. An anti-viral drug should be effective against both current and future variants. Additionally, timing and dosage of treatment should be optimised to reduce the development of resistance. There have been varied reports for the efficacy of Molnupiravir in mixed target populations. Therefore, we have further characterised Molnupiravir by evaluating its activity in two different cell lines and identifying if delays in treatment lead to sub-optimal activity. Furthermore, we evaluated the effect of repeated exposure of SARS-CoV-2 to Molnupiravir.

106 **2.0 Materials and Methods**

107

108 **2.1 Compound**

109 NHC (Alsachim) was supplied as a 1mg powder (purity 95%) and was resuspended in 1ml
110 DMSO to provide a 4.07mM stock solution. This was diluted in viral maintenance media
111 (DMEM containing 2% FBS and 0.05mg/ml gentamicin) for experiments using a range of
112 concentrations.

113

114 **2.2 Cell culture**

115 Human ACE2-A549 (hACE2-A549 were the kind gift of Oliver Schwartz (Buchrieser et al.,
116 2020). These were cultured in DMEM with 10% FBS and 0.05mg/ml gentamicin with the
117 addition of 10µg/ml Blasticidin (Invitrogen). Only passage 3-10 cultures were used for
118 experiments. Calu-3 cells (HTB-55; ATCC) were cultured in DMEM with 10% FBS and
119 0.05mg/ml gentamicin. Vero/hSLAM cells (PHE) were grown in DMEM with 10% FBS and
120 0.05mg/ml gentamicin (Merck) with the addition of 0.4mg/ml Geneticin (G418;
121 Thermofisher) at 37°C/5% CO_2.

122

123 **2.3 Viral Culture**

124 Virus stocks were grown in Vero/hSLAM cells using DMEM containing 2% FBS, 0.05mg/ml
125 gentamicin and 0.4mg/ml geneticin and harvested 72 hours post inoculation. Virus stocks
126 were aliquoted and stored at -80°C. The titre of stocks (PFU/ml) was determined by plaque
127 assay. RNA from viral stocks were sequenced by Oxford Nanopore long read length
128 sequencing on flow cells run on GridION.

129

130 **2.4 Sequencing of viral stocks**

131 Sequencing libraries for ARTIC amplicons were prepared following the 'PCR tiling of SARS-
132 CoV-2 virus with Native Barcoding' protocol provided by Oxford Nanopore Technologies
133 using LSK109 and EXP-NBD196. The artic-ncov2019 pipeline v1.2.1
134 (https://artic.network/ncov-2019/ncov2019-bioinformatics-sop.html) was used to filter
135 the passed fastq files produced by Nanopore sequencing with read lengths between 400
136 nt and 700 nt for ARTIC amplicons. This pipeline was then used to map the filtered reads
137 on the reference SARS-CoV-2 genome (MN908947.3) by minimap2 and assigned each read
138 alignment to a derived amplicon and excluded primer sequences based on the ARTIC V3
139 and V4 primer schemes in the bam files. Primer-trimmed bam files were further analysed
140 using DiversiTools (http://josephhughes.github.io/DiversiTools/) with the "-orfs" function
141 to generate the ratio of amino acid change in the reads and coverage at each site of protein
142 in comparison to the reference SARS-CoV-2 genome (MN908947.3). The amino acids with
143 highest ratio and coverage > 10 were used to assemble the consensus protein sequences.
144 Pangolin (https://pangolin.cog-uk.io/) was used to confirm lineages of each viral stock
145 used in experiments.

146

147 **2.5 *In-vitro* cytotoxicity of NHC**

148 Human ACE2-A549 cells and Calu-3 cells were plated at 2 x 10^4 cells per well in a clear
149 bottomed white 96 well plate. Twenty-four hours later the medium was replaced with
150 media containing NHC at different concentrations. At 72 hours post-exposure, cell viability
151 was measured by CellTiter-Glo assay (Promega) as per the manufacturer's instructions.

152

153

154 **2.5 Anti-viral activity of NHC against SARS-CoV-2 Variants of Concern (VoCs)**

155 Human ACE2-A549 cells and Calu-3 cells were grown to confluency and infected at an MOI
156 (Multiplicity of Infection) of 0.1 in either DMEM with 2% FBS and 0.05mg/ml gentamicin,
157 or in the same media containing 0.01µM, 0.1µM, 1µM or 10µM NHC by allowing virus to
158 adsorb to cells in a volume of 100µl for one hour at 37°C, and then topping up to 500µl
159 with the relevant media afterwards. A mock infected control and a DMSO control were
160 included in each experiment and experiments were repeated a minimum of 3 times. After
161 72 hours, supernatants were collected and stored at -80°C until viral titre was determined
162 by plaque assay. The inhibitory potency of NHC measured as the absolute IC50 was defined
163 as the concentration of drug that resulted in a 50% reduction in the number of plaques
164 compared to untreated controls.

165

166 **2.6 Pre-exposure and Post-exposure to NHC**

167 For pre-exposure experiments, media was removed from hACE2-A549 cells and replaced
168 with media containing NHC two hours prior to infection. This was then removed for
169 infection, which was performed as described above. For concomitant and post-exposure
170 experiments, infections were performed in media as described above. At two, four, 24 or
171 48 hours post-infection and concomitant infection media was removed from cells. The cells
172 were washed twice with PBS, and the media replaced with media containing 0µM, 0.01µM,
173 0.1µM, 1µM or 10µM NHC NHC. After 72 hours post-infection, supernatants were
174 collected and stored at -80°C until viral titre was determined by plaque assay.

175

176

177

178 **2.7 Serial Passage experiments for detection of resistance**

179 To determine if Molnupiravir resistance would occur through repeated exposure to low
180 doses of the drug, SARS-CoV-2 was passaged every 2-3 days in Calu-3 cells in either the
181 presence or absence of the approximate IC50 of the drug (0.1µM). Passaging was done by
182 taking 100µl of the supernatant and adding it to fresh cells for one hour at 37°C before
183 topping up with the relevant media. At passages 1, 5, 15 and 20 the supernatant was
184 collected, titred by plaque assay, and (i) used to perform dose response assays to the drug
185 (as previously described) at an MOI of 0.01 for each passage and (ii) RNA extracted and
186 NimaGen-illumina sequencing performed. An illustration of the experimental outline if
187 provided in figure 1.

188

189

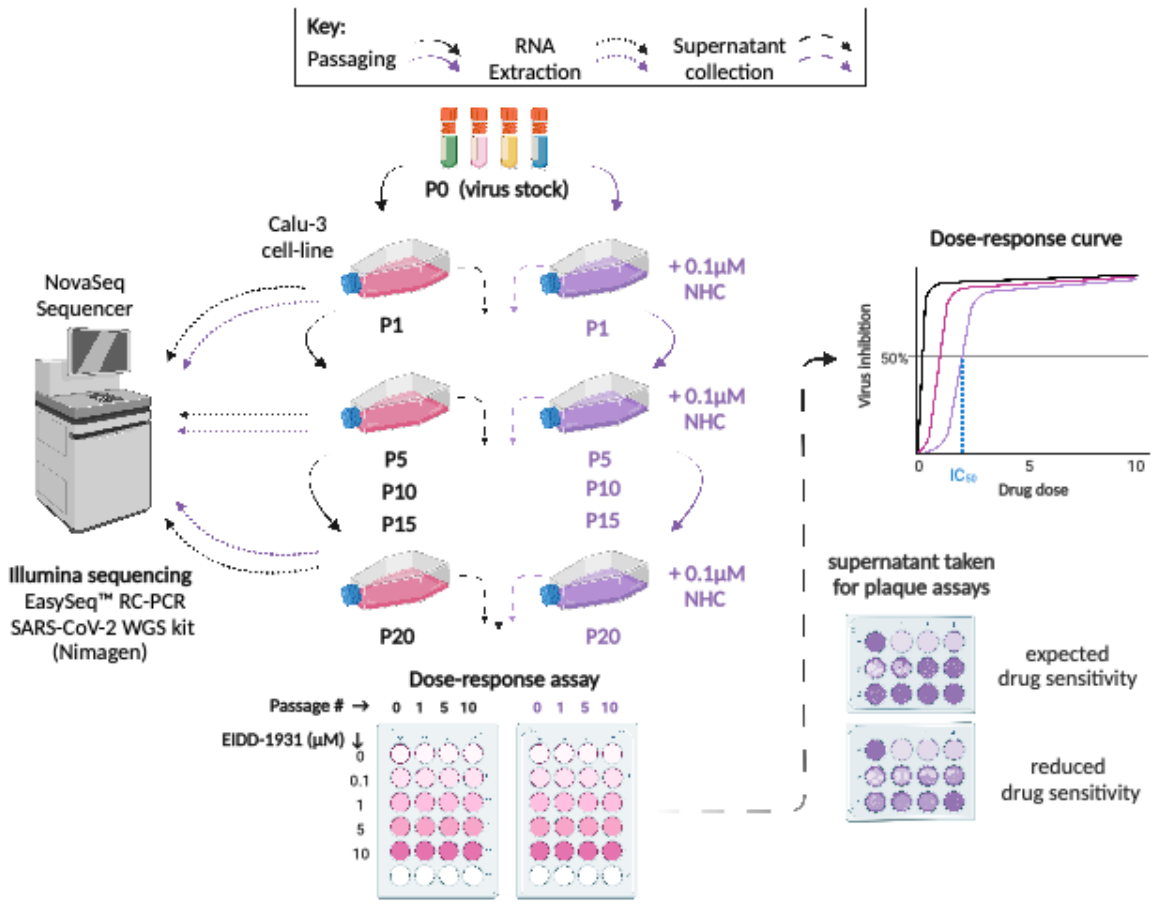

Figure 1. Experimental outline for measurement of resistance of SARS-CoV-2 to NHC. Calu-3 cells were infected with SARS-CoV-2 at an MOI of 0.01 in either the presence or absence of the approximate IC50 of the drug (0.1µM) and then passaged every 2-3 days. Virus was passaged by taking 100µl of the supernatant and adding it to fresh cells for one hour at 37°C before topping up with the relevant media with or without NHC. At passages 1, 5, 15 and 20 the supernatant was collected, titred by plaque assay, and (i) used to perform dose response assays to the drug (as previously described) at an MOI of 0.01 for each passage and (ii) RNA extracted and NimaGen-illumina sequencing performed.

2.8 NimaGen-Illumina Sequencing and Bioinformatic analysis

NimaGen libraries were prepared and amplified as described previously before being sequenced on the NovaSeq 6000 machine. Bioinformatic analysis was likewise performed as previously described (Donovan-Banfield et al., 2022). Briefly, the raw sequencing data was processed using two different pipelines. The first pipeline, EasySeq_covid19 (version

206 0.9, code available at https://github.com/JordyCoolen/easyseq_covid19), performs
207 quality control steps, maps to the reference genome (Wuhan-Hu-1; NC045512.2
208 https://www.ncbi.nlm.nih.gov/nuccore/NC_045512.2), variant calls and generates a
209 consensus genome for each sample (Coolen et al., 2021). Default parameters were used
210 and are as follows: variant call threshold = 0.5; variant calling quality threshold = 20; variant
211 calling minimum depth = 10. Pangolin (version 4.0.6) was used to assign SARS-CoV-2
212 lineage, with maximum ambiguity set at 0.31 (https://pangolin.cog-uk.io/) (O'Toole et al.,
213 2021). The second method, DiversiTools (code available at
214 https://github.com/josephhughes/DiversiTools), uses the primer-trimmed alignment file
215 (named as [sampleID]_L001.final.bam) and its associated index file (produced in the
216 EasySeq pipeline) along with the reference genome and a coding region file to analyse the
217 minor genomic variation and predict the amino acid sequence based on the genomic data.
218 DiversiTools allows for an in-depth analysis of viral diversity in each sample, rather than
219 just the consensus/dominant genomic information. Data visualisation was conducted in R
220 (version 4.0.2), using the tidyverse package (version 1.3.2) for data manipulation. All plots
221 were created using ggplot2 (version 3.3.6). Figures were compiled using cowplot (version
222 1.1.1) and magick (version 2.7.3) packages. Data and code are available at
223 https://doi.org/10.5281/zenodo.7594012.
224
225 **2.9 Statistical analysis**
226 A one-way ANOVA with post-hoc Tukey test was used to evaluate the *in-vitro* cytotoxicity
227 data. For dose response curves, the absolute IC50 values were calculated using GraphPad
228 Prism 9.5, using a non-linear 4-parameter logistic regression. An extra sum-of-squares F-
229 test was used to determine if there was any evidence that that the data sets in each

230 logistic regression differed from each other. T-tests comparing the IC50 values for hACE2-
231 A549 cells and Calu-3 cells were used to determine if the IC50 values differed between
232 cell lines. As an additional analysis, a one-way ANOVA was performed on the recorded
233 IC50 values for the serial passaging experiment. P was considered significant if <0.05 and
234 a minimum of three replicates was performed for each experiment. All plots were created
235 using GraphPad Prism 9.5 and figure 1 was created using Biorender.com.
236
237

238 **3.0 Results and Discussion**

239 To find the appropriate non-toxic concentration range of NHC in hACE2-A549 and Calu-3
240 cells, Cell-titer Glo Assays (Promega) were used to measure % ATP production in cells. These
241 were treated with DMSO or different concentrations of NHC diluted in culture medium
242 compared to mock untreated cells. There was a slight increase (105.9%) in the ATP production
243 in cells at the lowest concentration of drug, 0.01µM ($p=0.02$) in hACE2-A549 cells. The only
244 concentration of drug to inhibit the ATP production was 10µM for both cell lines
245 (89.74±1.03%, and 81.2 ± 1.6%, $p>0.0001$) (Supplementary Figure 1a and b). However, cell
246 monolayers appeared completely intact, and therefore this dose was used as the upper limit
247 in the dose response assays.

248

249 **3.1 NHC has equivalent efficiency against different VOCs *in vitro***

250 NHC has been evaluated against different VOCs in various cell lines, with its IC50 (the
251 concentration of drug required to reduce the amount of live virus by 50%) reported between
252 0.08-10µM (Bojkova et al., 2022; Lee et al., 2021; Rosenke et al., 2021; Sheahan et al., 2020;
253 Stegmann et al., 2021; Zhou et al., 2021). Therefore, before we could determine the
254 treatment window, we needed to determine what the IC50 was in our cell lines and if it was
255 equivalent for different VOCs. Molnupiravir, as a nucleoside analogue, acts by mimicking
256 naturally occurring nucleosides to create error catastrophe during virus replication in the
257 host. Therefore, due to its random nature, we would expect this compound to act against all
258 variants of the virus in a similar manner as it does not target any specific region of the virus.
259 Dose response assays were performed by infecting hACE2-A549 and Calu-3 cells at an MOI of
260 0.1 in media alone and in media containing 0.01, 0.1, 1, and 10µM NHC. After 72 hours,
261 supernatants were removed, and viral titres determined by plaque assay. The IC50 was

262 determined using a 4-parameter non-linear regression with GraphPad Prism 9.5. IC50 values
263 were similar for each variant in hACE2-A549 cells of 0.1µM, while there was more variation
264 observed in Calu-3 cells, ranging from 0.11 to 0.38µM in different variants. T-tests revealed
265 that there was no significant difference between the IC50 for each VOC in either cell line
266 (p>0.05) and an extra sum-of-squares F-test revealed that there was no significant difference
267 between the best-fit curves for hACE2-A549 cells (p=0.99) and Calu-3 cells (p=0.16) (Table 1,
268 Figure 2). Interestingly Delta had a slightly elevated IC50 compared to the other VOCs (though
269 not statistically significant), which has been noted before in a Roborovski dwarf hamster
270 model (Lieber et al., 2022).

Variant	**hACE2-A549**	**Calu-3**	**T-test results**
	IC50 (µM)	**IC50 (µM)**	**(P-value)**
Liverpool/REMRQ0001/2020 (B lineage)	0.11	0.16	P=0.24
Alpha (B.1.1.7)	0.1	0.11	P=0.41
Beta (B.1.351)	0.13	0.18	P=0.54
Delta (B.1.617.2)	0.1	0.38	P=0.66

271
272 **Table 1. IC50 values of NHC against variants in human lung cell models.** Inhibitory activity of
273 NHC against an early variant of SARS-CoV-2 (Liverpool/REMRQ0001/2020) and Alpha
274 (B.1.1.7), Beta (B.1.351) and Delta (B.1.617.2) variants of concern (VOCs). A four-parameter
275 non-linear regression was used to calculate the IC50 for each variant (n=4) and T-tests used
276 to compare the IC50 for each VOC across cell-lines.
277

A

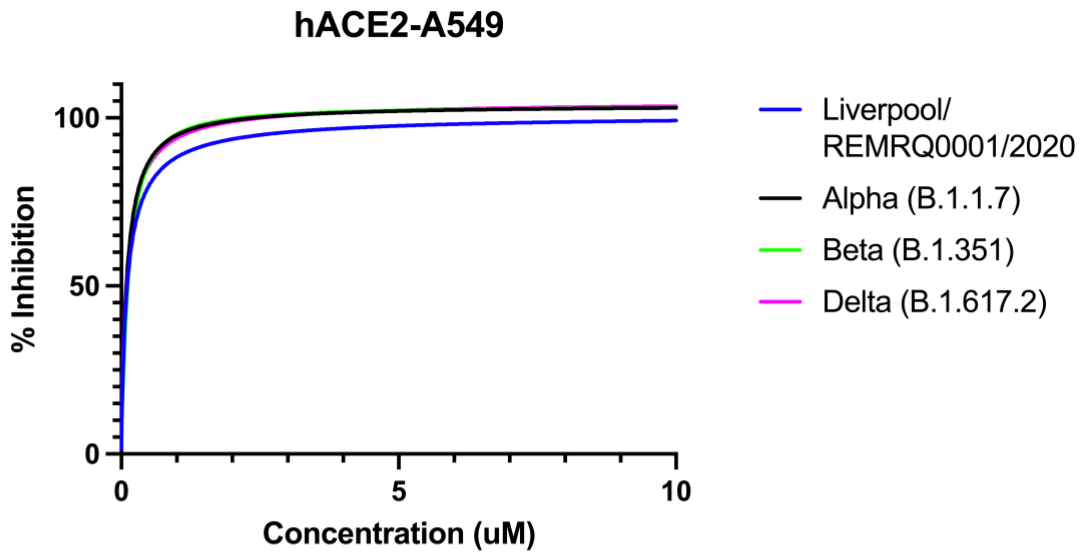

B

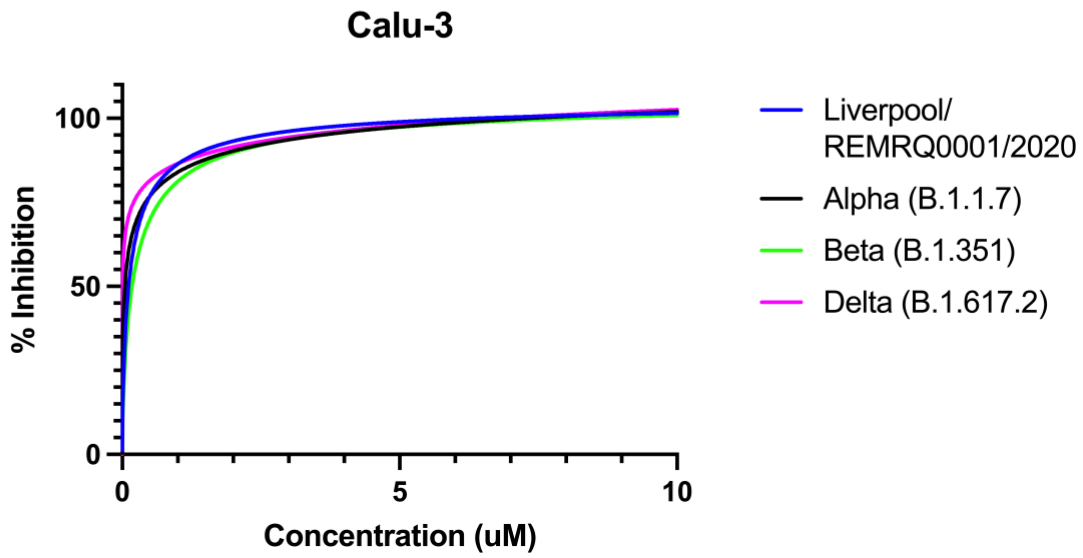

Figure 2. NHC is similarly active against both an early variant and VOCs in A) hACE2-A549 cells and B) Calu-3 cells. Inhibitory activity of NHC against an early variant of SARS-CoV-2 (Liverpool/REMRQ001/2020) and Alpha (B.1.1.7), Beta (B.1.351) and Delta (B.1.617.2) variants of concern (VOCs). A non-linear regression was used to plot the dose response curves and calculate the IC50 for each variant (n=4).

285 **3.2 The ability of NHC to inhibit the growth of SARS-CoV-2 VOCs is dependent on timing of**
286 **administration**

287 To determine the effective treatment window, hACE2-A549 cells were both pre-
288 treated with different concentrations of NHC two hours prior to infection and treated at two,
289 four, 24- and 48-hours post-infection and compared to concurrent treatment/infection. Dose-
290 response assays were performed on supernatants collected 72 hours post-infection. Viral
291 titres remained similar if treatment was given prior to, or at the same time as infection and
292 at time points of two, four- and 24-hours post-infection. However, if treatment was given at
293 48 hours post-infection, the drug was not as effective for all variants tested with inhibition
294 never reaching 100% (Figure 3). An extra sum-of squares F-test was performed for each
295 variant and demonstrated that the curves differed significantly for Liverpool ($P=0.0018$),
296 Alpha ($P<0.001$), Beta ($P=0.0008$) but a p-value could not be calculated for Delta.
297
298

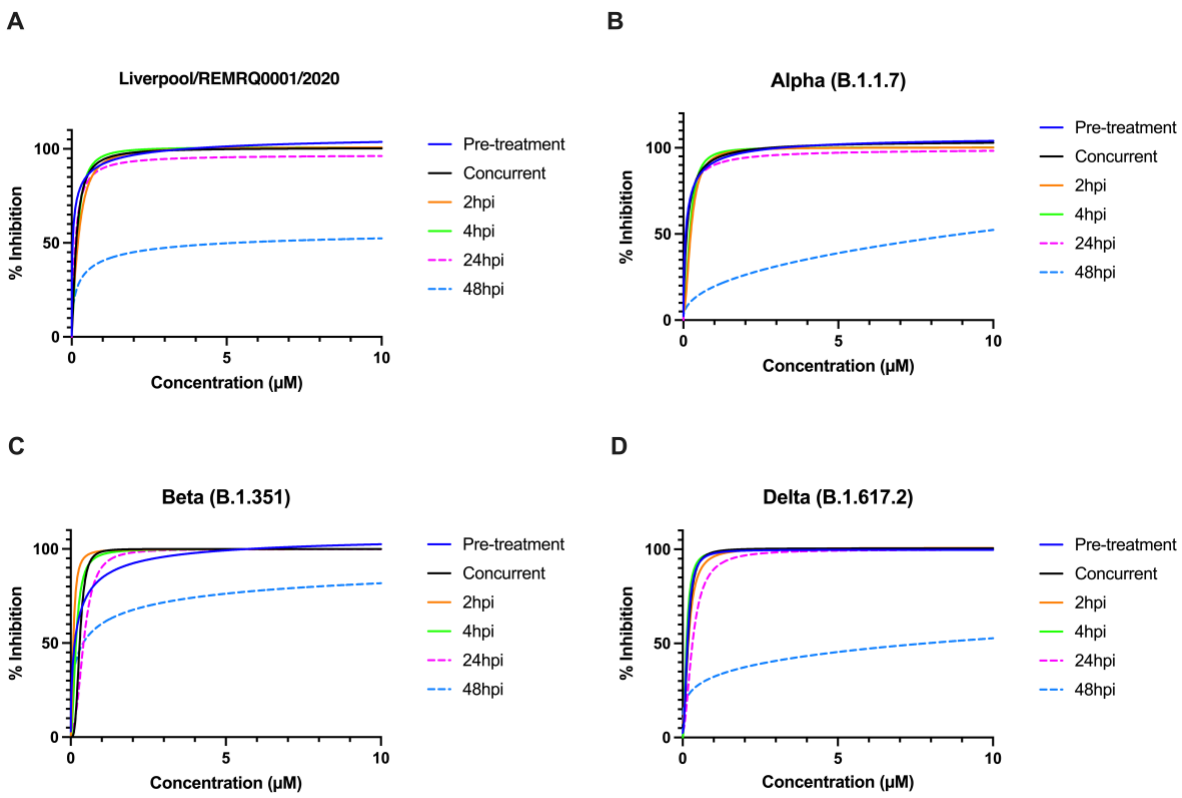

Figure 3. Effect of pre-treatment, concurrent treatment and treatment at two, four, 24 and 48 hours post-infection on inhibition of viral growth in hACE2-A549 cells. Dose response assays were performed on supernatants collected 72 hours post-infection for (A) the Liverpool variant, (B) Alpha (B.1.1.7), (C) Beta (B.1.351) or (D) Delta (B.1.617.2) variants. A non-linear regression was used to plot the dose response curves for each variant (n=3).

These results have been borne out by others using a hollow-fibre injection model (Brown et al., 2022) and in animal models (Abdelnabi et al., 2021; Rosenke et al., 2021). Virological and pathological analysis in patients who died of severe COVID-19 suggested that by the time immunopathology is recognised, giving an anti-viral in the expectation that this would reduce symptoms associated with COVID-19 is too late (Dorward et al., 2021). While the large clinical studies on patients receiving Molnupiravir claim patients were given the drug within five days of symptoms, few have directly measured the effect of delays in treatment post-symptom onset. A weak relationship (not statistically significant) between disease onset time and administration of Molnupiravir was identified in a single centre observational study

315 in Poland. A delay in Molnupiravir administration was associated with an increase in the
316 likelihood of hospitalisation (Czarnecka et al., 2022). Furthermore a recent Italian study in
317 patients > 80 years old found that the greater the number of days from the onset of symptoms
318 to administration of therapy, the higher the likelihood was of hospitalisation or death (Bruno
319 et al., 2022). These results indicate that the relative muted effects of Molnupiravir given to
320 patients in real world settings may be the result of delayed administration of the drug.
321
322 **3.3 A fixed dose exposure to the IC50 of NHC did not induce resistance after 20 passages for**
323 **Beta, but results were inconclusive for the Liverpool variant**
324 Anti-viral drugs are being used to treat patients with persistent infection, particularly
325 in patients who have compromised immunity. In this setting, Molnupiravir may be given over
326 extended periods of time. Therefore, to determine if drug-induced adaptations to NHC were
327 likely to emerge after prolonged exposure, Calu-3 cells were infected in either the presence
328 of a sub-optimal dose of NHC (0.1µM) or in media alone, with two variants, the
329 Liverpool/REMRQ0001/2020 (B lineage), and the Beta VOC (B.1.351). These viruses were
330 passaged 20 times and supernatants were titred and analysed by NHC dose response assays
331 every five passages in order to determine if the IC50 had changed.
332 For the Liverpool variant, logistic regression curves for each passage were plotted. An
333 extra sum-of squares F-test suggested that the curves differed (p=0.019) (Figure 4a). The
334 percent inhibition values are plotted in Figure 4b with the mean +/- SEM. To explore this
335 further, the IC50 values for each replicate were plotted and an ordinary one-way ANOVA with
336 post-hoc Tukey test was performed to determine if there was any significant change over the
337 course of passage. This found no significant differences in the IC50 values between any
338 pairwise combination (p=0.55) (Figure 4c).

339 Dose response results for the Beta variant were analysed by logistic regression and
340 likewise plotted with the extra sum-of-squares F-test but the result demonstrated no
341 difference between the curves (p=0.66) (Figure 4d). The percent inhibition values are plotted
342 in Figure 4e with the mean +/- SEM. The IC50 were similarly plotted, and the ANOVA revealed
343 there was no significant difference between any pairwise combination (p=0.28) (Figure 4f).

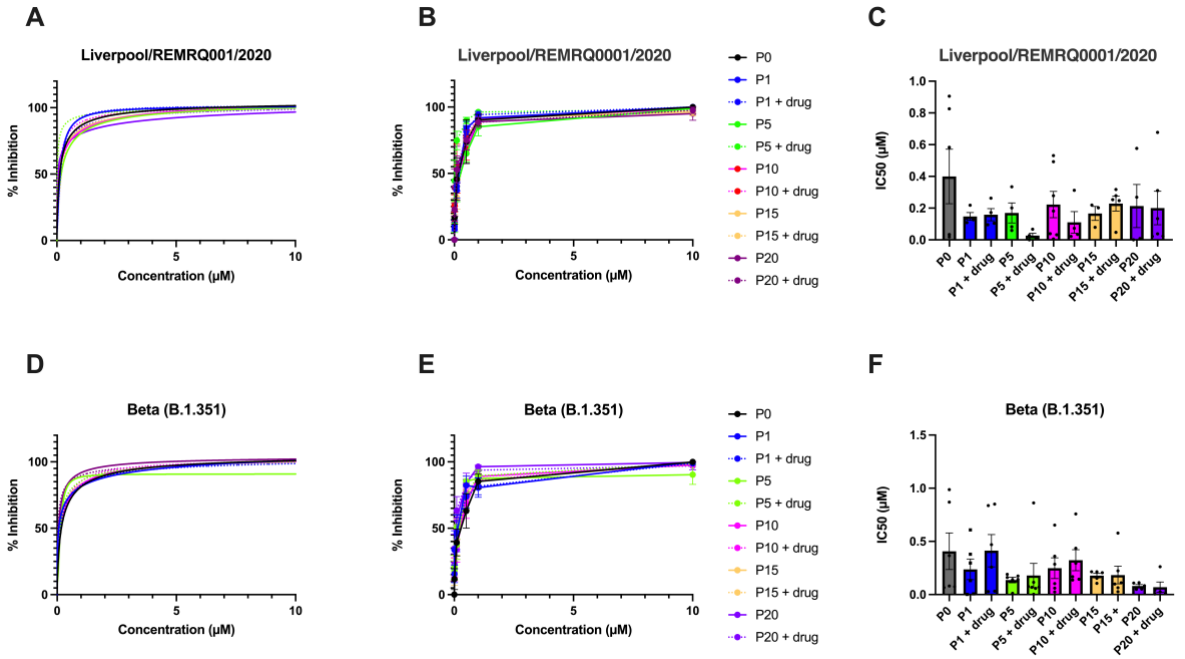

344

345 **Figure 4. A fixed dose exposure to the IC50 of NHC did not induce resistance after 20**
346 **passages for Beta, but results were inconclusive for the Liverpool variant.** (A) Logistic
347 regression curves for the Liverpool variant. (B) Percentage inhibition values plotted for each
348 passage (mean ± SEM) for the Liverpool variant. (C) IC50 values plotted for each passage
349 (mean ± SEM) for the Liverpool variant (n>/=3). (D) Logistic regression curves for the Beta
350 VOC. (E) Percentage inhibition values plotted for each passage (mean ± SEM) for the Beta
351 VOC. (F) IC50 values plotted for each passage (mean ± SEM) for the Beta VOC (n>/=5).
352

353 While the results for the Liverpool variant were inconclusive, the Beta variant showed
354 no signs of resistance. Although our methods differ, most studies agree that Molnupiravir
355 has a high genetic barrier to resistance in viruses, such as VEEV (Urakova et al.,
356 2018)Influenza, RSV (Yoon et al., 2018) or MERS (Agostini et al., 2019). However, more studies
357 should be performed in animal models to better delineate this.

358 All anti-virals currently approved for use against SARS-CoV-2 have their limitations and
359 Molnupiravir is no exception. While results suggesting that earlier administration could
360 improve the efficacy of the drug in real-world scenarios have been confirmed by others,
361 Brown et al (2022) have suggested increasing the dose of the drug 5-fold could overcome
362 delays to therapy. However, tolerability in patients could be an issue and higher doses are not
363 recommended due to concerns over host mutagenicity (Zhou et al., 2021).
364

365 **3.4 Sequencing of serially passaged virus revealed that the hallmark of Molnupiravir**
366 **treatment was detectable *in vitro.***

367 Molnupiravir acts to cause error catastrophe through the induction of transition
368 mutations (e.g. C -> U or G -> A changes). We hypothesised that if this were the case, that
369 there would have been an increase in the proportion of transition to transversion mutations
370 with treatment, compared to control. To investigate this, one sample for each condition was
371 taken forward to measure the transition/transversion ratio in the genome of SARS-CoV-2
372 during serial passage (figure 5). The data indicated that repeated exposure to NHC (e.g. in
373 passaging) had a cumulative effect on the mean transition/transversion ratio for both variants
374 tested. At p1, the mean transition/transversion ratio for untreated Liverpool virus was 0.18,
375 increasing to 0.37 at p20 while for NHC treated virus the ratio went from 0.2 to 0.83. For the
376 beta variant, the mean transition/transversion ratio in untreated samples increased from 0.43
377 at P1 to 0.48 at P20 while NHC treated virus increased from 0.42 to 0.88.

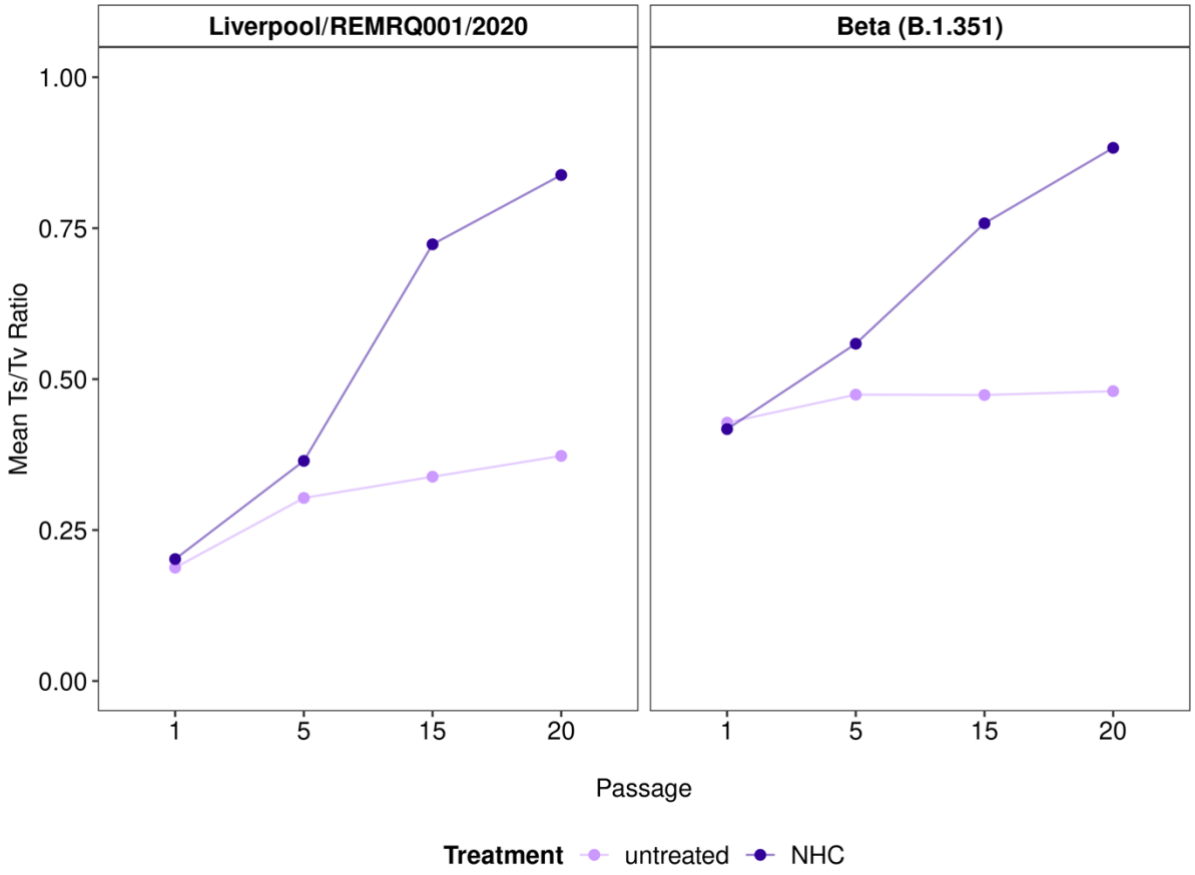

Figure 5. The mean transition/transversion ratio for each passaged virus. Graphs plotting the mean transition/transversion ratio (Ts/Tv) for each virus for untreated and NHC treated viruses at each passage (n=1).

3.5 An analysis of the non-synonymous and synonymous amino acid changes revealed that there was little difference between untreated and NHC treated viruses.

To investigate the selection pressure of Molnupiravir on different viral proteins, an analysis of the predicted amino-acid changes relative to the length of each viral protein was performed. (Figure 6a and b). Transition mutations are less likely to result in non-synonymous amino-acid substitutions (Stoltzfus and Norris, 2015), so Molnupiravir would most likely cause synonymous amino acid substitutions. We did not observe any preferential regions in the genome that had an increased frequency of either synonymous or non-synonymous amino-acid substitutions in NHC treated cells compared to untreated.

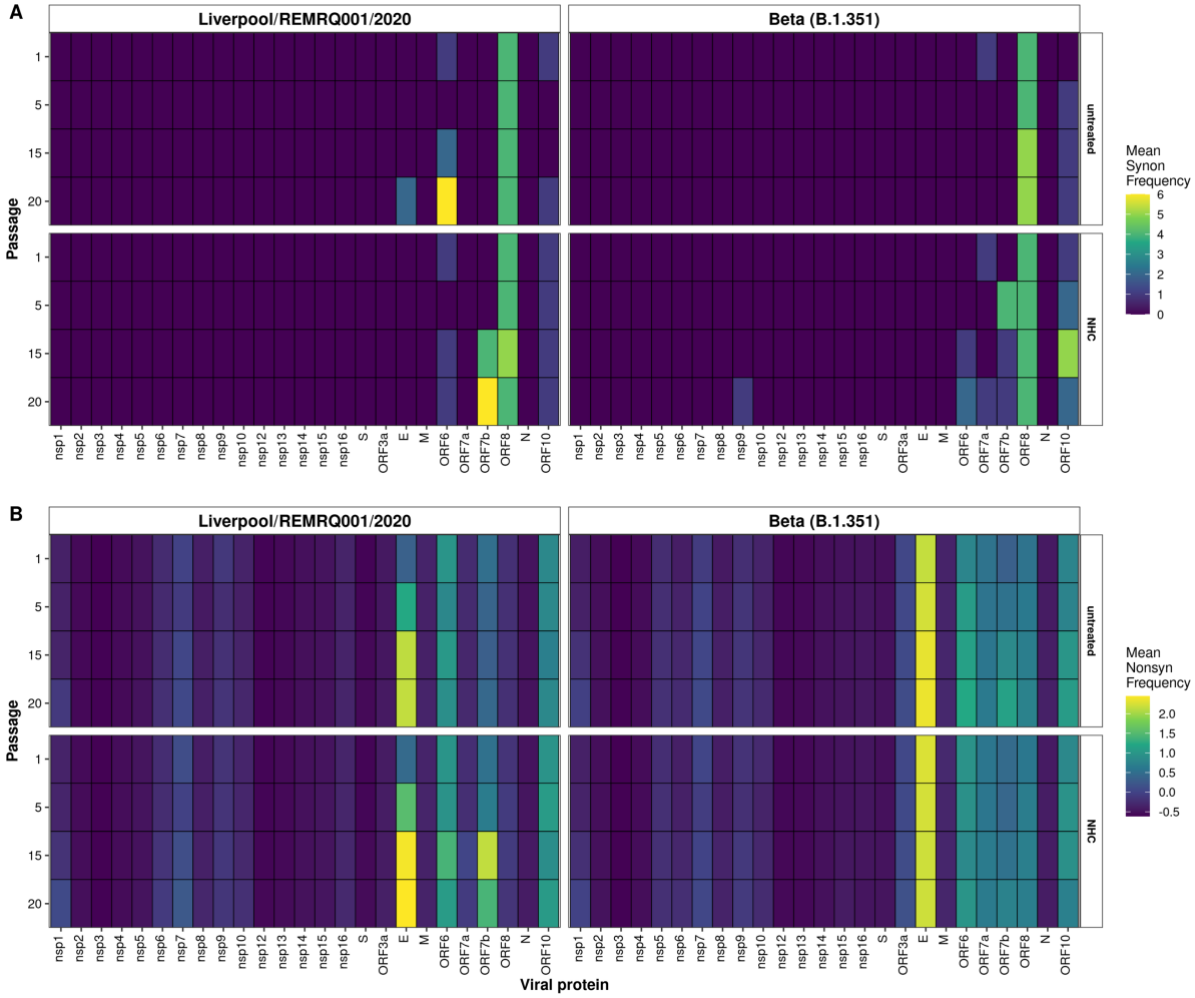

Figure 6. The frequency of amino acid changes relative to length of viral protein between treated and untreated viruses. Figures show the frequency (%) of amino-acid changes relative to the length of protein for each passage for both treated and untreated viruses. A) Synonymous amino acid changes. B) Non-synonymous amino acid changes. Data is missing for p10 untreated Liverpool variant (n=1).

We propose that the lack of observed resistance is due to the random nature of the drug's mechanism of action. However, recently scientists have suggested that Molnupiravir could lead to the generation of new variants through the same mechanism (Focosi, 2022). In our work we have shown that serial passage of virus in the presence of drug resulted in a cumulative increase in the transition to transversion ratio (Figure 5). This has been noted in patients from the AGILE trial (Donovan-Banfield et al., 2022), and elsewhere it induced a number of SNPs in the viral genome which increased over time. However these SNPs were

406 random and rarely persisted across timepoints suggesting there is less risk of the emergence
407 of new variants (Alteri et al., 2022).

408 Administering the drug when patients first display symptoms may not reduce viral
409 loads sufficiently to prevent disease. Based on the *in vitro* data, we hypothesize that
410 Molnupiravir should be given to patients as close to exposure as possible or prophylactically.
411 This is similar to the anti-viral philosophy underpinning the treatment of influenza infection
412 or pre-exposure prophylaxis for HIV. In agreement with our analysis of patients treated with
413 Molnupiravir (Donovan-Banfield et al., 2022), no changes in the predicted amino acid
414 sequence of SARS-CoV-2 was observed between treated and untreated conditions. However,
415 when SARS-CoV-2 was serially passaged with Molnupiravir, viable virus was recovered at each
416 stage with an increased mutational landscape. This emphasises that whatever the treatment
417 option in whatever patient category, if Molnupiravir is to be used, the dose given must be
418 sufficient to eliminate virus there and then. The implication of this observation is that in
419 persistently infected individuals, treatment should be such that virus is eliminated
420 immediately or risk increased mutational frequency. We predict that SARS-CoV-2 genomes
421 derived from cells that received Molnupiravir will have higher Ts/Tv ratios and at a population
422 level these may be distinguishable during genomic surveillance.

423

424 **Declaration of competing interest:**

425 The authors declare no competing interests.

426 **Acknowledgments** Virus isolates used in this study were originally derived from samples
427 gathered under the auspices of the ISARIC Coronavirus Clinical Characterisation Consortium

(ISARIC4C) and processed at the University of Liverpool. We would like to acknowledge all members of the consortium.

Funding: This work was funded by U.S. Food and Drug Administration Medical Countermeasures Initiative contract (75F40120C00085) awarded to JAH. The article reflects the views of the authors and does not represent the views or policies of the FDA. This work was also supported by the MRC (MR/W005611/1) G2P-UK: A national virology consortium to address phenotypic consequences of SARS-CoV-2 genomic variation (co-I JAH). For the purpose of Open Access, the authors have applied a CC BY public copyright license to any Author Accepted Manuscript version arising from this submission.

Author contributions. Conceptualization: TP, SK and JAH. Methodology: TP, ID-B, HG and RP-R. Validation: TP. Formal analysis: TP, ID-B, HG, RP-R and JAH. Investigation: TP. Resources: SK and JAH. Data Curation: TP, ID-B, HG and RP-R. Writing – original draft: TP and JAH. Writing – Review and Editing: All authors. Visualisation: TP. Supervision: TF, SK and JAH. Project administration: JAH. Funding acquisition: TF and JAH.

Bibliography

Abdelnabi, R., Foo, C.S., Kaptein, S.J.F., Zhang, X., Do, T.N.D., Langendries, L., Vangeel, L., Breuer, J., Pang, J., Williams, R., Vergote, V., Heylen, E., Leyssen, P., Dallmeier, K., Coelmont, L., Chatterjee, A.K., Mols, R., Augustijns, P., De Jonghe, S., Jochmans, D., Weynand, B., Neyts, J., 2021. The combined treatment of Molnupiravir and Favipiravir results in a potentiation of antiviral efficacy in a SARS-CoV-2 hamster infection model. EBioMedicine 72, 103595.

Agostini, M.L., Pruijssers, A.J., Chappell, J.D., Gribble, J., Lu, X., Andres, E.L., Bluemling, G.R., Lockwood, M.A., Sheahan, T.P., Sims, A.C., Natchus, M.G., Saindane, M., Kolykhalov, A.A., Painter, G.R., Baric, R.S., Denison, M.R., 2019. Small-Molecule Antiviral β-d-N(4)-Hydroxycytidine Inhibits a Proofreading-Intact Coronavirus with a High Genetic Barrier to Resistance. J Virol 93.

455 Alteri, C., Fox, V., Scutari, R., Burastero, G.J., Volpi, S., Faltoni, M., Fini, V., Granaglia, A.,
456 Esperti, S., Gallerani, A., Costabile, V., Fontana, B., Franceschini, E., Meschiari, M., Campana,
457 A., Bernardi, S., Villani, A., Bernaschi, P., Russo, C., Guaraldi, G., Mussini, C., Perno, C., 2022.
458 Genomic Evolution of Sars-Cov-2 in Molnupiravir-Treated Patients Compared to Paxlovid-
459 Treated and Drug-Naïve Patients: A Proof-of-Concept Study. Research Square.

460 Bojkova, D., Widera, M., Ciesek, S., Wass, M.N., Michaelis, M., Cinatl, J., 2022. Reduced
461 interferon antagonism but similar drug sensitivity in Omicron variant compared to Delta
462 variant of SARS-CoV-2 isolates. Cell Research 32, 319-321.

463 Brown, A., N., Lang, Y., Zhou, J., Franco Evelyn, J., Hanrahan Kaley, C., Bulitta Juergen, B.,
464 Drusano George, L., 2022. Why Molnupiravir Fails in Hospitalized Patients. mBio 0, e02916-
465 02922.

466 Bruno, G., Perelli, S., Giotta, M., Bartolomeo, N., De Vita, G., Buccoliero, G.B., 2022. Efficacy
467 and safety of oral antivirals in individuals aged 80 years or older with mild-to-moderate
468 COVID-19: preliminary report from an Italian Prescriber Center. Infez Med 30, 547-554.

469 Buchrieser, J., Dufloo, J., Hubert, M., Monel, B., Planas, D., Rajah, M.M., Planchais, C.,
470 Porrot, F., Guivel-Benhassine, F., Van der Werf, S., Casartelli, N., Mouquet, H., Bruel, T.,
471 Schwartz, O., 2020. Syncytia formation by SARS-CoV-2-infected cells. The EMBO Journal 39,
472 e106267.

473 Butler, C.C., Hobbs, F.D.R., Gbinigie, O.A., Rahman, N.M., Hayward, G., Richards, D.B.,
474 Dorward, J., Lowe, D.M., Standing, J.F., Breuer, J., Khoo, S., Petrou, S., Hood, K., Nguyen-
475 Van-Tam, J.S., Patel, M.G., Saville, B.R., Marion, J., Ogburn, E., Allen, J., Rutter, H., Francis,
476 N., Thomas, N.P.B., Evans, P., Dobson, M., Madden, T.-A., Holmes, J., Harris, V., Png, M.E.,
477 Lown, M., van Hecke, O., Detry, M.A., Saunders, C.T., Fitzgerald, M., Berry, N.S., Mwandigha,
478 L., Galal, U., Mort, S., Jani, B.D., Hart, N.D., Ahmed, H., Butler, D., McKenna, M., Chalk, J.,
479 Lavallee, L., Hadley, E., Cureton, L., Benysek, M., Andersson, M., Coates, M., Barrett, S.,
480 Bateman, C., Davies, J.C., Raymundo-Wood, I., Ustianowski, A., Carson-Stevens, A., Yu, L.-M.,
481 Little, P., Agyeman, A.A., Ahmed, T., Allcock, D., Beltran-Martinez, A., Benedict, O.E., Bird,
482 N., Brennan, L., Brown, J., Burns, G., Butler, M., Cheng, Z., Danson, R., de Kare-Silver, N.,
483 Dhasmana, D., Dickson, J., Engamba, S., Fisher, S., Fox, R., Frost, E., Gaunt, R., Ghosh, S.,
484 Gilkar, I., Goodman, A., Granier, S., Howell, A., Hussain, I., Hutchinson, S., Imlach, M., Irving,
485 G., Jacobsen, N., Kennard, J., Khan, U., Knox, K., Krasucki, C., Law, T., Lee, R., Lester, N.,
486 Lewis, D., Lunn, J., Mackintosh, C.I., Mathukia, M., Moore, P., Morton, S., Murphy, D., Nally,
487 R., Ndukauba, C., Ogundapo, O., Okeke, H., Patel, A., Patel, K., Penfold, R., Poonian, S.,
488 Popoola, O., Pora, A., Prasad, V., Prasad, R., Razzaq, O., Richardson, S., Royal, S., Safa, A.,
489 Sehdev, S., Sevenoaks, T., Shah, D., Sheikh, A., Short, V., Sidhu, B.S., Singh, I., Soni, Y.,
490 Thalasselis, C., Wilson, P., Wingfield, D., Wong, M., Woodall, M.N.J., Wooding, N., Woods, S.,
491 Yong, J., Yongblah, F., Zafar, A., 2022. Molnupiravir plus usual care versus usual care alone
492 as early treatment for adults with COVID-19 at increased risk of adverse outcomes
493 (PANORAMIC): an open-label, platform-adaptive randomised controlled trial. The Lancet.

494 Coolen, J.P.M., Wolters, F., Tostmann, A., van Groningen, L.F.J., Bleeker-Rovers, C.P., Tan, E.,
495 van der Geest-Blankert, N., Hautvast, J.L.A., Hopman, J., Wertheim, H.F.L., Rahamat-
496 Langendoen, J.C., Storch, M., Melchers, W.J.G., 2021. SARS-CoV-2 whole-genome

497 sequencing using reverse complement PCR: For easy, fast and accurate outbreak and variant
498 analysis. J Clin Virol 144, 104993.

499 Cox, M., Peacock, T.P., Harvey, W.T., Hughes, J., Wright, D.W., Willett, B.J., Thomson, E.,
500 Gupta, R.K., Peacock, S.J., Robertson, D.L., Carabelli, A.M., Consortium, C.-G.U., 2022. SARS-
501 CoV-2 variant evasion of monoclonal antibodies based on in vitro studies. Nature Reviews
502 Microbiology.

503 Cox, R.M., Wolf, J.D., Plemper, R.K., 2021. Therapeutically administered ribonucleoside
504 analogue MK-4482/EIDD-2801 blocks SARS-CoV-2 transmission in ferrets. Nat Microbiol 6,
505 11-18.

506 Czarnecka, K., Czarnecka, P., Tronina, O., Durlik, M., 2022. Molnupiravir Outpatient
507 Treatment for Adults with COVID-19 in a Real-World Setting—A Single Center
508 Experience, Journal of Clinical Medicine.

509 Donovan-Banfield, I.a., Penrice-Randal, R., Goldswain, H., Rzeszutek, A.M., Pilgrim, J.,
510 Bullock, K., Saunders, G., Northey, J., Dong, X., Ryan, Y., Reynolds, H., Tetlow, M., Walker,
511 L.E., FitzGerald, R., Hale, C., Lyon, R., Woods, C., Ahmad, S., Hadjiyiannakis, D., Periselneris,
512 J., Knox, E., Middleton, C., Lavelle-Langham, L., Shaw, V., Greenhalf, W., Edwards, T., Lalloo,
513 D.G., Edwards, C.J., Darby, A.C., Carroll, M.W., Griffiths, G., Khoo, S.H., Hiscox, J.A., Fletcher,
514 T., 2022. Characterisation of SARS-CoV-2 genomic variation in response to Molnupiravir
515 treatment in the AGILE Phase IIa clinical trial. Nature Communications 13, 7284.

516 Dorward, D.A., Russell, C.D., Um, I.H., Elshani, M., Armstrong, S.D., Penrice-Randal, R.,
517 Millar, T., Lerpiniere, C.E.B., Tagliavini, G., Hartley, C.S., Randle, N.P., Gachanja, N.N., Potey,
518 P.M.D., Dong, X., Anderson, A.M., Campbell, V.L., Duguid, A.J., Al Qsous, W., BouHaidar, R.,
519 Baillie, J.K., Dhaliwal, K., Wallace, W.A., Bellamy, C.O.C., Prost, S., Smith, C., Hiscox, J.A.,
520 Harrison, D.J., Lucas, C.D., 2021. Tissue-Specific Immunopathology in Fatal COVID-19. Am J
521 Respir Crit Care Med 203, 192-201.

522 Fischer, W.A., Eron, J.J., Holman, W., Cohen, M.S., Fang, L., Szewczyk, L.J., Sheahan, T.P.,
523 Baric, R., Mollan, K.R., Wolfe, C.R., Duke, E.R., Azizad, M.M., Borroto-Esoda, K., Wohl, D.A.,
524 Coombs, R.W., Loftis, A.J., Alabanza, P., Lipansky, F., Painter, W., 2021. A Phase 2a clinical
525 trial of Molnupiravir in patients with COVID-19 shows accelerated SARS-CoV-2 RNA
526 clearance and elimination of infectious virus. Science Translational Medicine 0, eabl7430.

527 Focosi, D., 2022. Molnupiravir: From Hope to Epic Fail?, Viruses.

528 Haddad, F., Dokmak, G., Karaman, R., 2022. A Comprehensive Review on the Efficacy of
529 Several Pharmacologic Agents for the Treatment of COVID-19, Life.

530 Jayk Bernal, A., Gomes da Silva, M.M., Musungaie, D.B., Kovalchuk, E., Gonzalez, A., Delos
531 Reyes, V., Martín-Quirós, A., Caraco, Y., Williams-Diaz, A., Brown, M.L., Du, J., Pedley, A.,
532 Assaid, C., Strizki, J., Grobler, J.A., Shamsuddin, H.H., Tipping, R., Wan, H., Paschke, A.,
533 Butterton, J.R., Johnson, M.G., De Anda, C., 2022. Molnupiravir for Oral Treatment of Covid-
534 19 in Nonhospitalized Patients. New England Journal of Medicine.

535 Jochmans, D., Liu, C., Donckers, K., Stoycheva, A., Boland, S., Stevens, S.K., De Vita, C.,
536 Vanmechelen, B., Maes, P., Trüeb, B., Ebert, N., Thiel, V., De Jonghe, S., Vangeel, L., Bardiot,
537 D., Jekle, A., Blatt, L.M., Beigelman, L., Symons, J.A., Raboisson, P., Chaltin, P., Marchand, A.,
538 Neyts, J., Deval, J., Vandyck, K., 2023. The substitutions L50F, E166A and L167F in SARS-CoV-
539 2 3CLpro are selected by a protease inhibitor in vitro; and confer resistance to nirmatrelvir.
540 mBio e02815-22.

541 Johnson, M.G., Strizki, J.M., Brown, M.L., Wan, H., Shamsuddin, H.H., Ramgopal, M.,
542 Florescu, D.F., Delobel, P., Khaertynova, I., Flores, J.F., Fouche, L.F., Chang, S.-C., Williams-
543 Diaz, A., Du, J., Grobler, J.A., Paschke, A., De Anda, C., 2023. Molnupiravir for the treatment
544 of COVID-19 in immunocompromised participants: efficacy, safety, and virology results from
545 the phase 3 randomized, placebo-controlled MOVe-OUT trial. Infection.

546 Kabinger, F., Stiller, C., Schmitzová, J., Dienemann, C., Kokic, G., Hillen, H.S., Höbartner, C.,
547 Cramer, P., 2021. Mechanism of Molnupiravir-induced SARS-CoV-2 mutagenesis. Nature
548 Structural & Molecular Biology.

549 Kearns, P., Siebert, S., Willicombe, m., Gaskell, C., Kirkham, A., Pirrie, S., Bowden, S.,
550 Magwaro, S., Hughes, A., Lim, Z., Dimitriadis, S., Murray, S.M., Marjot, T., Win, Z., Irwin, S.L.,
551 Meacham, G., Richter, A.G., Kelleher, P., Satsangi, J., Miller, P., Rea, D., Cook, G., Turtle, L.,
552 Klenerman, P., Dunachie, S., Basu, N., de Silva, T.I., Thomas, D., Barnes, E., Goodyear, C.S.,
553 McInnes, I., 2021. Examining the Immunological Effects of COVID-19 Vaccination in Patients
554 with Conditions Potentially Leading to Diminished Immune Response Capacity – The
555 OCTAVE Trial. , Preprintes with The Lancet.

556 Khoo, S.H., FitzGerald, R., Saunders, G., Middleton, C., Ahmad, S., Edwards, C.J.,
557 Hadjiyiannakis, D., Walker, L., Lyon, R., Shaw, V., Mozgunov, P., Periselneris, J., Woods, C.,
558 Bullock, K., Hale, C., Reynolds, H., Downs, N., Ewings, S., Buadi, A., Cameron, D., Edwards, T.,
559 Knox, E., Donovan-Banfield, I.a., Greenhalf, W., Chiong, J., Lavelle-Langham, L., Jacobs, M.,
560 Northey, J., Painter, W., Holman, W., Lalloo, D.G., Tetlow, M., Hiscox, J.A., Jaki, T., Fletcher,
561 T., Griffiths, G., Paton, N., Hayden, F., Darbyshire, J., Lucas, A., Lorch, U., Freedman, A.,
562 Knight, R., Julious, S., Byrne, R., Cubas Atienzar, A., Jones, J., Williams, C., Song, A., Dixon, J.,
563 Alexandersson, A., Hatchard, P., Tilt, E., Titman, A., Doce Carracedo, A., Chandran Gorner,
564 V., Davies, A., Woodhouse, L., Carlucci, N., Okenyi, E., Bula, M., Dodd, K., Gibney, J., Dry, L.,
565 Rashid Gardner, Z., Sammour, A., Cole, C., Rowland, T., Tsakiroglu, M., Yip, V., Osanlou, R.,
566 Stewart, A., Parker, B., Turgut, T., Ahmed, A., Starkey, K., Subin, S., Stockdale, J., Herring, L.,
567 Baker, J., Oliver, A., Pacurar, M., Owens, D., Munro, A., Babbage, G., Faust, S., Harvey, M.,
568 Pratt, D., Nagra, D., Vyas, A., 2022. Molnupiravir versus placebo in unvaccinated and
569 vaccinated patients with early SARS-CoV-2 infection in the UK (AGILE CST-2): a randomised,
570 placebo-controlled, double-blind, phase 2 trial. The Lancet Infectious Diseases.

571 Kokic, G., Hillen, H.S., Tegunov, D., Dienemann, C., Seitz, F., Schmitzova, J., Farnung, L.,
572 Siewert, A., Höbartner, C., Cramer, P., 2021. Mechanism of SARS-CoV-2 polymerase stalling
573 by remdesivir. Nature Communications 12, 279.

574 Lee, J., Lee, J., Kim, H.J., Ko, M., Jee, Y., Kim, S., 2021. TMPRSS2 and RNA-dependent RNA
575 polymerase are effective targets of therapeutic intervention for treatment of COVID-19
576 caused by SARS-CoV-2 variants (B.1.1.7 and B.1.351). Microbiol Spectr 9, e0047221.

Lieber, C.M., Cox, R.M., Sourimant, J., Wolf, J.D., Juergens, K., Phung, Q., Saindane, M.T., Smith, M.K., Sticher, Z.M., Kalykhalov, A.A., Natchus, M.G., Painter, G.R., Sakamoto, K., Greninger, A.L., Plemper, R.K., 2022. SARS-CoV-2 VOC type and biological sex affect Molnupiravir efficacy in severe COVID-19 dwarf hamster model. Nature Communications 13, 4416.

Moghadasi, S.A., Heilmann, E., Moraes, S.N., Kearns, F.L., von Laer, D., Amaro, R.E., Harris, R.S., 2022. Transmissible SARS-CoV-2 variants with resistance to clinical protease inhibitors. bioRxiv.

O'Toole, Á., Scher, E., Underwood, A., Jackson, B., Hill, V., McCrone, J.T., Colquhoun, R., Ruis, C., Abu-Dahab, K., Taylor, B., Yeats, C., du Plessis, L., Maloney, D., Medd, N., Attwood, S.W., Aanensen, D.M., Holmes, E.C., Pybus, O.G., Rambaut, A., 2021. Assignment of epidemiological lineages in an emerging pandemic using the pangolin tool. Virus Evolution 7.

Rosenke, K., Hansen, F., Schwarz, B., Feldmann, F., Haddock, E., Rosenke, R., Barbian, K., Meade-White, K., Okumura, A., Leventhal, S., Hawman, D.W., Ricotta, E., Bosio, C.M., Martens, C., Saturday, G., Feldmann, H., Jarvis, M.A., 2021. Orally delivered MK-4482 inhibits SARS-CoV-2 replication in the Syrian hamster model. Nature Communications 12, 2295.

Sheahan, T.P., Sims, A.C., Zhou, S., Graham, R.L., Pruijssers, A.J., Agostini, M.L., Leist, S.R., Schäfer, A., Dinnon, K.H., Stevens, L.J., Chappell, J.D., Lu, X., Hughes, T.M., George, A.S., Hill, C.S., Montgomery, S.A., Brown, A.J., Bluemling, G.R., Natchus, M.G., Saindane, M., Kolykhalov, A.A., Painter, G., Harcourt, J., Tamin, A., Thornburg, N.J., Swanstrom, R., Denison, M.R., Baric, R.S., 2020. An orally bioavailable broad-spectrum antiviral inhibits SARS-CoV-2 in human airway epithelial cell cultures and multiple coronaviruses in mice. Science Translational Medicine 12, eabb5883.

Stegmann, K.M., Dickmanns, A., Heinen, N., Groß, U., Görlich, D., Pfaender, S., Dobbelstein, M., 2021. N4-hydroxycytidine and inhibitors of dihydroorotate dehydrogenase synergistically suppress SARS-CoV-2 replication. bioRxiv, 2021.2006.2028.450163.

Stoltzfus, A., Norris, R., 2015. On the Causes of Evolutionary Transition:Transversion Bias. Molecular biology and evolution 33.

Szemiel, A.M., Merits, A., Orton, R.J., MacLean, O.A., Pinto, R.M., Wickenhagen, A., Lieber, G., Turnbull, M.L., Wang, S., Furnon, W., Suarez, N.M., Mair, D., da Silva Filipe, A., Willett, B.J., Wilson, S.J., Patel, A.H., Thomson, E.C., Palmarini, M., Kohl, A., Stewart, M.E., 2021. In vitro selection of Remdesivir resistance suggests evolutionary predictability of SARS-CoV-2. PLOS Pathogens 17, e1009929.

Urakova, N., Kuznetsova, V., Crossman, D.K., Sokratian, A., Guthrie, D.B., Kolykhalov, A.A., Lockwood, M.A., Natchus, M.G., Crowley, M.R., Painter, G.R., Frolova, E.I., Frolov, I., 2018. β-d-N(4)-Hydroxycytidine Is a Potent Anti-alphavirus Compound That Induces a High Level of Mutations in the Viral Genome. J Virol 92.

Wahl, A., Gralinski, L.E., Johnson, C.E., Yao, W., Kovarova, M., Dinnon, K.H., 3rd, Liu, H., Madden, V.J., Krzystek, H.M., De, C., White, K.K., Gully, K., Schäfer, A., Zaman, T., Leist, S.R.,

617 Grant, P.O., Bluemling, G.R., Kolykhalov, A.A., Natchus, M.G., Askin, F.B., Painter, G.,
618 Browne, E.P., Jones, C.D., Pickles, R.J., Baric, R.S., Garcia, J.V., 2021. SARS-CoV-2 infection is
619 effectively treated and prevented by EIDD-2801. Nature 591, 451-457.

620 Yoon, J.J., Toots, M., Lee, S., Lee, M.E., Ludeke, B., Luczo, J.M., Ganti, K., Cox, R.M., Sticher,
621 Z.M., Edpuganti, V., Mitchell, D.G., Lockwood, M.A., Kolykhalov, A.A., Greninger, A.L.,
622 Moore, M.L., Painter, G.R., Lowen, A.C., Tompkins, S.M., Fearns, R., Natchus, M.G., Plemper,
623 R.K., 2018. Orally Efficacious Broad-Spectrum Ribonucleoside Analog Inhibitor of Influenza
624 and Respiratory Syncytial Viruses. Antimicrob Agents Chemother 62.

625 Zhou, S., Hill, C.S., Sarkar, S., Tse, L.V., Woodburn, B.M.D., Schinazi, R.F., Sheahan, T.P., Baric,
626 R.S., Heise, M.T., Swanstrom, R., 2021. β-d-N4-hydroxycytidine Inhibits SARS-CoV-2 Through
627 Lethal Mutagenesis But Is Also Mutagenic To Mammalian Cells. The Journal of Infectious
628 Diseases 224, 415-419.

629 Zhou, Y., Gammeltoft, K.A., Ryberg, L.A., Pham, L.V., Fahnøe, U., Binderup, A., Hernandez,
630 C.R.D., Offersgaard, A., Fernandez-Antunez, C., Peters, G.H.J., Ramirez, S., Bukh, J.,
631 Gottwein, J.M., 2022. Nirmatrelvir Resistant SARS-CoV-2 Variants with High Fitness in Vitro.
632 Science Advances 8.
633